

Article

## Targeting Heterogeneous Tumors Using a Multifunctional Molecular Prodrug

Amit Sharma, Min-Goo Lee, Miae Won, Seyoung Koo, Jonathan F. Arambula, Jonathan L. Sessler, Sung-Gil Chi, and Jong Seung Kim

*J. Am. Chem. Soc.*, **Just Accepted Manuscript** • DOI: 10.1021/jacs.9b07171 • Publication Date (Web): 11 Sep 2019

Downloaded from [pubs.acs.org](https://pubs.acs.org) on September 11, 2019

### Just Accepted

“Just Accepted” manuscripts have been peer-reviewed and accepted for publication. They are posted online prior to technical editing, formatting for publication and author proofing. The American Chemical Society provides “Just Accepted” as a service to the research community to expedite the dissemination of scientific material as soon as possible after acceptance. “Just Accepted” manuscripts appear in full in PDF format accompanied by an HTML abstract. “Just Accepted” manuscripts have been fully peer reviewed, but should not be considered the official version of record. They are citable by the Digital Object Identifier (DOI®). “Just Accepted” is an optional service offered to authors. Therefore, the “Just Accepted” Web site may not include all articles that will be published in the journal. After a manuscript is technically edited and formatted, it will be removed from the “Just Accepted” Web site and published as an ASAP article. Note that technical editing may introduce minor changes to the manuscript text and/or graphics which could affect content, and all legal disclaimers and ethical guidelines that apply to the journal pertain. ACS cannot be held responsible for errors or consequences arising from the use of information contained in these “Just Accepted” manuscripts.

# Targeting Heterogeneous Tumors Using a Multifunctional Molecular Prodrug

Amit Sharma,<sup>†,‡</sup> Min-Goo Lee,<sup>§,‡</sup> Miae Won,<sup>†</sup> Seyoung Koo,<sup>†</sup> Jonathan F. Arambula,<sup>Ψ</sup> Jonathan L. Sessler<sup>\*,⊥,Ψ</sup> Sung-Gil Chi,<sup>\*,§</sup> and Jong Seung Kim<sup>\*,†</sup>

<sup>†</sup> Department of Chemistry, Korea University, Seoul 02841 Korea.

<sup>§</sup> Department of Life Sciences, Korea University, Seoul 02841, Korea.

<sup>⊥</sup> Institute for Supramolecular Chemistry and Catalysis, Shanghai University, Shanghai 200444, China.

<sup>Ψ</sup> Department of Chemistry, University of Texas at Austin, Austin, TX 78712-1224, USA.

<sup>‡</sup> These authors contributed equally.

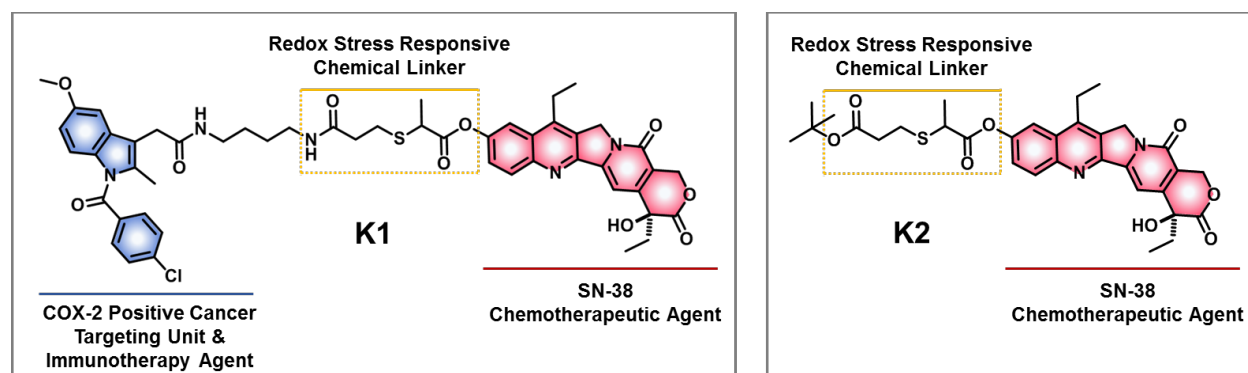
**ABSTRACT:** Reported here is a molecular construct (**K1**) designed to overcome hurdles associated with delivering active drugs to heterogeneous tumor environments. Construct **K1** relies on two cancer environment triggers (GSH & H<sub>2</sub>O<sub>2</sub>) to induce prodrug activation. It releases an active drug form (SN-38) under conditions of both oxidative and reductive stress *in vitro*. Specific uptake of **K1** in COX-2 positive aggressive colon cancer cells (SW620 and LoVo) was seen, along with enhanced anticancer activity compared with the control agent SN-38. These findings are attributed to environmentally triggered drug release, as well as simultaneous scavenging of species giving rise to intracellular redox stress. **K1** serves to downregulate various cancer survival signaling pathways (AKT, p38, IL-6, VEGF, and TNF- $\alpha$ ) and upregulate an anti-inflammatory response (IL-10). Compared with SN-38 and DMSO as controls, **K1** also displayed an improved *in vivo* therapeutic efficacy in a xenograft tumor regrowth model with no noticeable systemic toxicity at the administered dose. We believe that the strategy described here presents an attractive approach to addressing solid tumors characterized by intratumoral heterogeneity.

## ■ INTRODUCTION

Owing to the high cost, long development times, and limited success rates associated with the development of new cancer therapeutics, alternative strategies involving modification of anticancer drugs approved by US Food and Drug Administration (FDA) are attractive.<sup>1</sup> Such modification efforts could minimize the recognized side-effects of the anticancer agents in question or improve their clinical efficacy. Ultimately, this could translate into improved outcomes, including prolonged cancer patient survival.<sup>2</sup> Particularly effective may be modification strategies that enhance the delivery of chemotherapeutic drugs to a target site of interest. To date, remarkable advances in understanding the intricate pathways responsible for malignant progression, as well a greater appreciation of cancer development, have translated into a number of innovative strategies for targeting cytotoxins to specific sites of interest.<sup>1,3,4</sup> Typically, this is done in a phenotype-specific fashion by conjugating a drug or prodrug to a carrier that takes advantage of disease-related biomarkers to effect targeting and release. This can minimize adverse side-effects, reduce required dose levels or evade some multidrug resistance mechanisms, such as membrane-associated p-glycoprotein mediated drug efflux.<sup>5,6</sup> To

date most carrier-drug conjugates targeting cancer have exploited stable but conditionally labile linkages that are sensitive to a single biological input, such as subphysiological pH, temperature, protease, glutathione, or hydrogen peroxide.<sup>7,8</sup> However, the biomarkers in question are rarely unique to cancerous sites, resulting in suboptimal selectivity and reduced overall therapeutic efficacy.<sup>9</sup> The concurrent use of different biological triggers may allow these limitations to be overcome.<sup>10</sup> However, care must be taken that the therapeutic agent being subject to masking/demasking for delivery is released ultimately in its unmodified active form so as to avoid challenges from the regulatory bodies.<sup>11,12</sup>

Colorectal cancer (CRC) is the third most frequently diagnosed cancer in the United States. Its global burden is expected to increase by 60% through 2030 in spite of large-scale initial screening efforts.<sup>13,14</sup> Complex pro-tumor inflammatory cascades and immune-mediated processes play roles in both CRC initiation and metastasis.<sup>15</sup> Irinotecan (also referred to as CPT) is a front-line clinically approved chemotherapy drug for colon cancer. It is converted to the active metabolite SN-38 by carboxylesterase-mediated hydrolysis of the bispiperidine moiety (present as a solubilizing functional group). This active form induces toxicity in cancer cells by forming a topoisomerase



**Scheme 1.** Design strategy underlying the proposed inflammation guided redox-responsive cancer prodrugs **K1** and **K2** that are the subject of the present study.

inhibitor-DNA complex, thereby affecting DNA functions. However, owing to its slow hydrolysis rate, CPT displays a 100- to 1000- fold lower cell-based toxicity than SN-38 with a correspondingly reduced level of therapeutic efficacy in humans.<sup>16</sup> Resistance to apoptotic cell death mechanisms has also been put forward as a reason for poor clinical outcomes in the case of CPT-based therapies.<sup>17</sup> It is our belief that these clinical deficiencies might be overcome in part by more effective targeting of the active SN-38 drug form to tumors.

One targeting strategy that is appealing involves the use of a COX-2 inhibitor. COX-2 is a key enzyme involved in the synthesis of tumor cell-derived prostaglandins (PGs). PGs and COX-2 serve both as pro-inflammatory mediators and immune suppressors of anticancer immunity.<sup>18,19</sup> Increased expression of COX-2 mRNA and PGs has been reported in various cancers, including breast, colorectal, lung, stomach and pancreatic cancers with these levels being correlated with poor survival outcomes in CRC patients.<sup>20</sup> Recently, COX-2 inhibitors have shown promise as antiangiogenic therapies, either alone or in combination with anticancer drugs; they have also been seen to inhibit VEGF-independent PG-induced tumor angiogenesis in preclinical models.<sup>21,22</sup> We, and others believe that COX-2 inhibitors could play a useful role as targeting agents, particularly in the case of heterogeneous tumors.<sup>23-26</sup> The present study was designed to test further this supposition and, in doing so, address through chemical means the problem of tumor heterogeneity.

Cancer cells are remarkably heterogeneous.<sup>27,28</sup> As compared to normal cells, many cancer cells exist in a strongly reducing environment due to elevated levels of intracellular glutathione (GSH). This feature is often exacerbated under conditions of chemotherapy.<sup>29</sup> In seeming contradiction, a number of cancers are characterized by oxidative stress due to the overproduction of various reactive oxygen species (ROS).<sup>30</sup> Elevated reductive and oxidative stress may exist in different tumors (inter-tumoral) and even co-exist at different progression stages within the same tumor (intra-tumoral) or at the sub-organelle level within the same cancer cell.<sup>31</sup> This heterogeneity can be manifest in terms of intra-tumoral redox potential differences. A few redox-based nano-strategies have been reported in an effort to address the problems associated with targeting heterogeneous tumor environments.<sup>32,33</sup> However, to our knowledge, a combined approach involving selective tumor targeting followed by activation of a therapeutic drug by specific molecular mechanisms has yet to be reported.

Here we detail the synthesis and study of a new molecularly targeted system (**K1**, Scheme 1) that is subject to activation using either reducing (GSH) or oxidative ( $H_2O_2$ ) inputs likely to

be present in the tumor microenvironment. This allows active delivery of an FDA approved drug, SN-38. Construct **K1** also incorporates indomethacin, a COX-2 inhibitor that has been utilized successfully to achieve tumor targeting and knockdown of inflammatory regulated immune-suppressive genes. The molecular combination embodied in **K1** (*i.e.*, SN-38 and indomethacin) was thus expected to be advantageous in addressing the problem of aggressive CRC where tumor heterogeneity, COX-2 related inflammation, and effective cancer-selective prodrug activation constitute recognized hurdles. Since **K1** incorporates multiple potentially useful subunits into a single construct, it might also offer benefits in terms of reduced off-target toxicity and control over drug pharmacokinetics and biodistribution effects. The present study was designed to test these hypotheses.

## RESULTS AND DISCUSSION

The motivation underlying the present study was a desire to develop a prodrug conjugate that would allow for i) cancer-selective drug delivery *in vivo* and ii) active agent release through more than one mechanism of action. Conjugate **K1** was designed with such objectives in mind. This system contains both an NSAID COX-2 inhibitor and an SN-38 active payload designed to effect tumor targeting and growth inhibition, respectively. It also contains a specific thioether that was expected to undergo cleavage when exposed to either GSH or  $H_2O_2$ .<sup>34</sup> The synthesis of prodrug **K1** is outlined in Scheme S1 (Supporting Information, SI). First, intermediate **3** was synthesized *via* a Michael addition reaction between 2-mercaptopropionic acid and *tert*-butyl acrylate. Intermediate **3** was coupled with the topoisomerase I inhibitor, 7-ethyl-10-hydroxyl-camptothecin (SN-38, active metabolite of irinotecan) through esterification using EDC/DMAP (EDC = 1-ethyl-3-(3-dimethylaminopropyl)carbodiimide; DMAP, 4-dimethylamino-pyridine) to furnish intermediate **K2** (*cf.* Scheme 1). Subsequent *tert*-butyl deprotection with TFA (trifluoroacetic acid) in methylene chloride and subsequent acid-amine coupling of intermediates **4** and **2** resulted in the formation of conjugate **K1** in good yield. All the intermediates and products were characterized by standard analytical means (*cf.* Supporting Information).

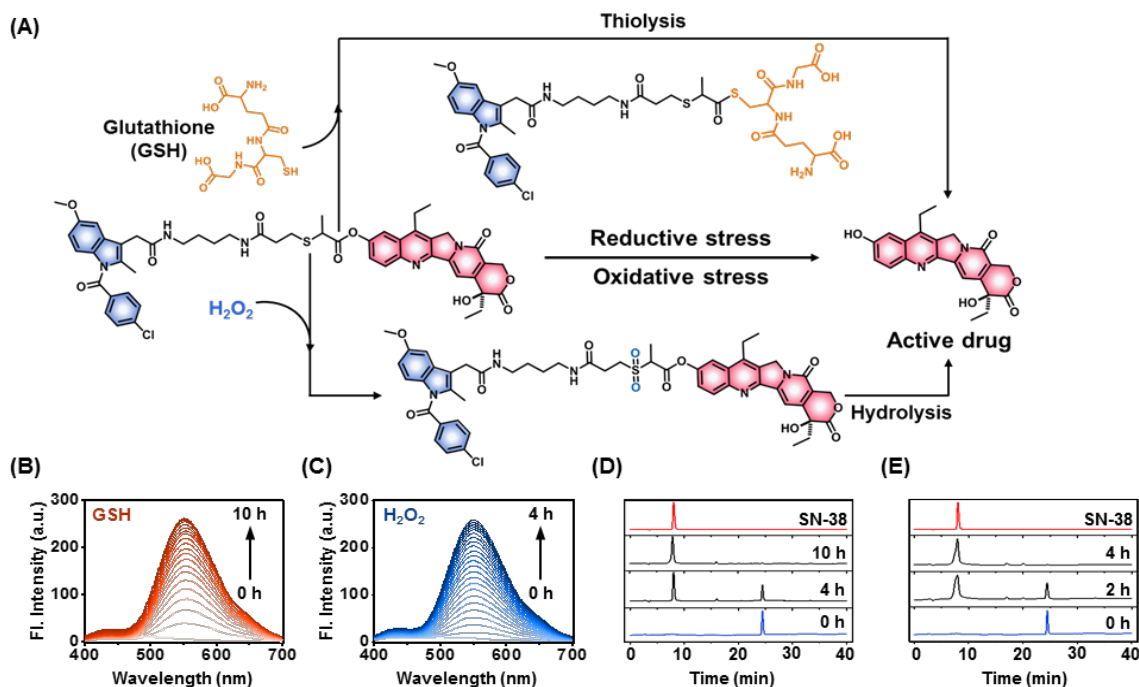


**Figure 1.** Proposed activation modes for prodrug **K1** expected to be operative under conditions of reductive and oxidative stress. (A) Under reductive stress, glutathione (GSH) undergoes thiolysis at the SN-38 linked ester functionality to form an intermediate with simultaneous release of active drug SN-38. Under oxidative stress, the sulfide functionality in the chemical linker is oxidized to a sulfone/sulfoxide moiety resulting in conversion of a hydrophobic site to a hydrophilic one that upon hydrolysis releases the active drug SN-38. Time-dependent fluorescence intensity change corresponding to SN-38 release upon incubation of **K1** (10  $\mu$ M) with (B) GSH (5 mM, 30 min) and (C) H<sub>2</sub>O<sub>2</sub> (0.125 mM, 10 min) in phosphate saline buffered (37  $^{\circ}$ C,  $\lambda_{\text{ex}}$  = 365 nm, Slit width 3/3). High-performance liquid chromatogram of **K1** (10  $\mu$ M) recorded at different time intervals following treatment with (D) GSH (5 mM), (E) H<sub>2</sub>O<sub>2</sub> (0.125 mM) and SN-38 in PBS (37  $^{\circ}$ C).

To investigate the drug release behavior of **K1** under model reductive (glutathione, GSH) and oxidative (hydrogen peroxide, H<sub>2</sub>O<sub>2</sub>) stress conditions, UV-Vis, fluorescence and high-performance liquid chromatography (HPLC) studies were carried out in phosphate-buffered saline (PBS, pH = 7.4) at 37  $^{\circ}$ C. **K1** proved largely stable in PBS until exposed to either H<sub>2</sub>O<sub>2</sub> or GSH as confirmed by fluorescence and HPLC analyses (Figure 1 & S1-3). An enhancement in the intensity of the UV-Vis absorbance band of **K1** at 365 nm was seen upon incubation with GSH (5 mM) and H<sub>2</sub>O<sub>2</sub> (0.125 mM) (Figure S2). Further, as shown in Figure 1B & 1C, **K1** gives rise to a weak emission band at 540 nm ( $\lambda_{\text{ex}}$  = 365 nm). When tested under model reductive stress prodrug activation conditions mimicking those expected under physiological conditions,<sup>29,30</sup> *i.e.*, incubation of **K1** with GSH (5 mM), an enhancement in the fluorescence intensity at 540 nm was observed. The fluorescence band at 540 nm is characteristic of free SN-38. Incubation with H<sub>2</sub>O<sub>2</sub> at levels deemed physiologically relevant<sup>29,35</sup> produced a similar enhancement in the overall fluorescence intensity (Figure 1C). We also tested the activation behavior of **K1** by monitoring the change in the fluorescence emission features upon exposure to different concentrations of GSH and H<sub>2</sub>O<sub>2</sub> (Figure S3).

Additional evidence for **K1** activation upon exposure to GSH and H<sub>2</sub>O<sub>2</sub> came from the combined high-performance liquid chromatography (HPLC) (Figure 1D&E) and electronic spray ionization mass spectrometry (ESI-MS) studies (Figures S4 and S5). **K1** is characterized by a retention peak at 24.5 min in the HPLC chromatogram under our conditions of analysis; however, incubation with GSH (5 mM) for 10 h, leads to formation of new peaks with retention times of 8.0 min (active drug SN-38) and 16 min (byproduct), respectively. These results are consistent with **K1** undergoing thiolysis (presumably mediated by

the -SH group of GSH) of the phenolic ester moiety to release free SN-38. Unlike other GSH responsive prodrugs, **K1** allows for direct release of an active drug form as the result of the concomitant consumption of GSH.<sup>7,36</sup> Separately, incubation of **K1** with H<sub>2</sub>O<sub>2</sub> (0.125 mM, 4 h) results in oxidation of the thioether moiety to the corresponding sulfone or sulfoxide. These latter putative intermediates are relatively hydrophilic, which is thought to abet hydrolysis. This proposed hydrolysis cleaves the phenolic ester present in **K1** and releases SN-38 in its free (active) form. A combination of UV-Vis, fluorescence, HPLC (Figure 1C & 1D) and ESI-MS analyses (Figures S4 S5) provide support for the proposed mechanism of **K1** activation shown in Figure 1A. The activation behavior of **K2** was also investigated (Figure S6). Finally, the stability of prodrugs **K1** and **K2** stability in human serum was examined. Briefly, we found that **K1** is essentially stable up to 24 h when incubated in at 37  $^{\circ}$ C in PBS in the presence of 30% human serum, whereas **K2** undergoes substantially hydrolysis to SN-38 over the same 24 h period when exposed to 10% human serum (Figure S7). Accordingly, the focus of the present study was on **K1** with **K2** being used as a control.

As noted above, **K1** is comprised of SN-38 (topoisomerase I inhibitor) and an indomethacin (COX-2 inhibitor) subunit that is proposed to provide targeting through interactions with COX-2 proteins upregulated in many tumor types. To assess this, we performed cell viability assays using human cell lines with variable expression of COX-2 protein so as to determine whether **K1** induces COX-2-dependent cytotoxic activity. In cells with low COX-2 expression (*i.e.*, Caco-2, DLD-1, Figure S8), treatment with **K1** or the simpler control system **K2** resulted in a slight decrease in proliferation relative to LoVo and SW620

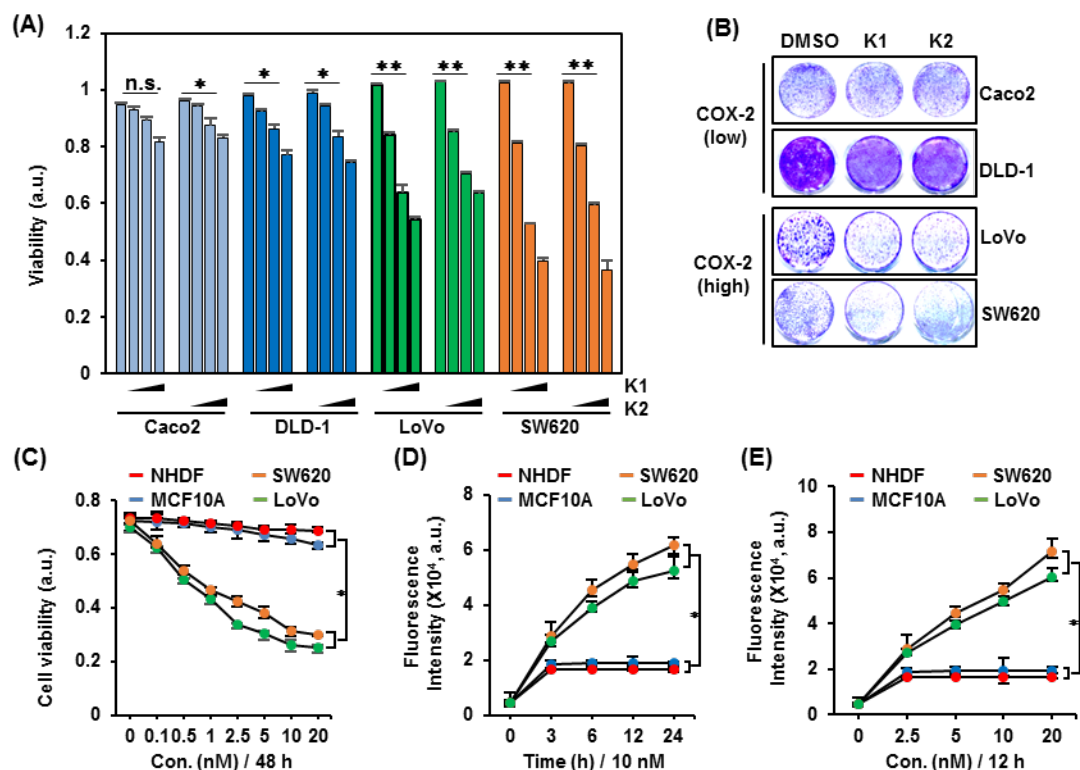


**Figure 2.** Effect of **K1** and **K2** on tumor cell viability and correlations with the expression status of COX-2. (A) Effect of **K1** and **K2** on cancer cell cytotoxicity. Cells were treated with **K1** and **K2** (0, 1, 5 and 10 nM) for 48 h. Cell viability was assessed by means of a WST-1 assay (mean  $\pm$  SD,  $n = 3$ , \* \*  $p < 0.01$ , \*  $p < 0.05$ , n.s., not significant). (B) Effect of **K1** and **K2** on cancer cell growth. Cells were treated with 1 nM **K1** or 1 nM **K2** for 5 days and were stained with crystal violet solution. (C) Effect of **K1** on cell viability in human normal and cancer cells. Cells were treated with the indicated doses of **K1** for 48 h. Cell viability was determined using a WST-1 assay (mean  $\pm$  SD,  $n = 3$ , \*  $p < 0.05$ ). (D & E) Comparative analysis of the extent of intracellular uptake of **K1** in human normal and cancer cells. Cells were treated for the indicated times and with the indicated doses of **K1**. Fluorescence intensities were determined using SpectraMAX I3.

cells characterized by increased COX-2 expression levels (Figure 2A & 2B).<sup>37</sup>

To assess further the COX-2 selectivity and anticancer potential of **K1**, additional cell viability assays were performed. These involved comparing COX-2 positive cancer cells (*i.e.*, LoVo, SW620) to healthy human cell lines NHDFs (normal human dermal fibroblasts) and MCF10A (human breast epithelial cell line) that have low COX-2 expression levels (Figure 2C, Figure S8). A positive correlation between the *in vitro* potency of **K1** and the COX-2 expression levels was seen. In addition, knockdown of endogenous COX-2 expression by means of siRNA COX-2 transfection in SW620 cells resulted in a reduction in the **K1**-induced cytotoxicity (Figure S9).

To assess whether **K1** displayed relatively enhanced cancer cell targeting, we examined the intracellular accumulation of **K1** in cancer cells (SW620, LoVo) and normal cells (NHDF & MCF10A). Treatment with **K1** gave rise to both a dose- and time-dependent induction in the cancer cells possessing higher COX-2 expression but not in the normal cells or cancer cells characterized by a low level of COX-2 expression (Figure 2D & 2E). These results provide support for the notion that the observed cytotoxic effects, as well as the fluorescence induction seen with **K1**, were highly dependent on COX-2 protein expression levels.

Previous studies have reported that high levels of antioxidants or free radical species alter the tumor redox status, resulting in drug resistance during cancer treatment.<sup>38</sup> The finding that treatment with H<sub>2</sub>O<sub>2</sub> and GSH under model conditions effected drug release from **K1** led us to infer that under *in vitro* conditions these or related redox-active species would induce

drug release from **K1** and that this would occur more effectively in the cancer cells due to differences in their concentrations relative to normal cells (Figure 1B & 1C). We thus tested whether **K1** could release the active drug in cancer cells under intracellular redox condition. For this study, LoVo cells were pretreated with *N*-acetylcysteine (NAC, a GSH precursor) and H<sub>2</sub>O<sub>2</sub> to induce changes in the cellular redox environment. The cells were then treated with **K1** and the release of SN-38 was monitored by monitoring the fluorescence emission. As expected, pretreatment with both H<sub>2</sub>O<sub>2</sub> and NAC increased significantly the fluorescence intensity, as expected for the release of SN-38 within these **K1**-treated cells (Figure 3A).

We further examined whether alterations in intracellular redox status would influence cell growth and the viability of cancer cells treated with **K1**. In the absence of redox stress, the effect of **K1** on cancer cell cytotoxicity was similar to that of SN-38. However, in NAC-pretreated cells, **K1** reduced cancer cell growth significantly as compared to treatment with SN-38 (Figures 3B, S10A). Similar results were seen in GSH (cellular antioxidant)-siRNA knock-downed cells in which treatment with **K1** reduced significantly cancer cell growth and cytotoxicity relative to SN-38 (Figure 3C, and Figure S10A). Similar results were obtained for **K1** in 3D-tumor spheroid models (LoVo cells) (Figure S11).

p38 Mitogen-activated protein kinase (MAPK) and protein kinase B (AKT) signaling are key pathways regulating cancer cell proliferation and apoptosis in response to redox status.<sup>39</sup> To understand the role that **K1** presumably has on cancer cell growth and survival under redox conditions considered relevant to those present in many cancerous locales, GSH knock down

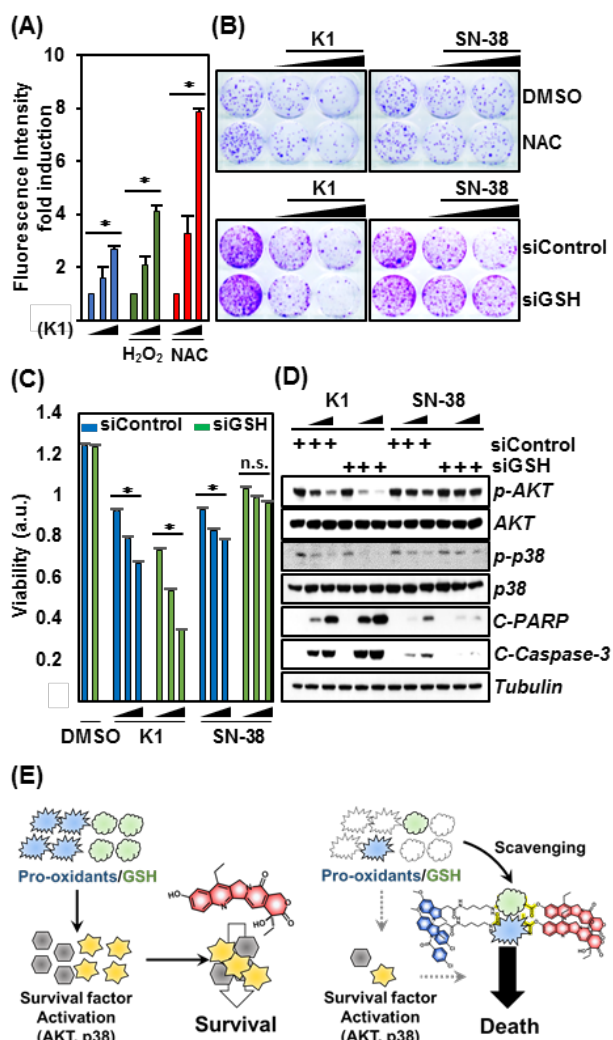


**Figure 3.** Effect of **K1** upon intracellular oxidative or reductive stress in LoVo cells. (A) Fluorescence intensity of **K1** in response to H<sub>2</sub>O<sub>2</sub> (50  $\mu$ M) and NAC (50  $\mu$ M) pretreatment (mean  $\pm$  SD,  $n = 3$ , \*  $p < 0.01$ ). (B) Effect of **K1** and SN-38 on cancer cell growth. LoVo cells were transfected with GSH siRNA or control siRNA and treated with NAC (50  $\mu$ M) and then treated with the indicated dose of **K1** and SN-38. Cells were stained with a solution of crystal violet. (C) Effect of **K1** and SN-38 on cancer cell cytotoxicity. LoVo cells were treated with **K1** and SN-38 (0, 5 and 10 nM) for 48 h. Cell viability was assessed by means of a WST assay (mean  $\pm$  SD,  $n = 3$ , \*  $p < 0.01$ ). (D) Effect of **K1** on cancer cell survival and apoptosis upon oxidative stress. Control or GSH knock-downed LoVo cells were treated with the indicated doses of **K1** and SN-38 for 48 h. The expression level of cancer survival proteins (phospho AKT and phospho p38) were determined by western blot. Cell apoptosis was measured by Western blot analysis of cleaved PARP and cleaved caspase-3. Tubulin was used as a protein loading control. (E) Schematic illustration of the cytotoxicity induced by **K1** in response to redox stress.

studies were conducted in LoVo cells so as to mimic cellular oxidative stress. These cells were then treated with either **K1** or

SN-38 and analyzed *via* western blot (Figure S10B). As shown in Figure 3D, treatment of control cells with **K1** or SN-38 resulted in a similar induction of cleavage of poly (ADP-ribose) polymerase (PARP) and caspase-3, and reduced phosphorylation of both p38 and AKT. In contrast, after GSH knockdown, **K1** treatment enhanced the induction of PARP and caspase-3 cleavage and strongly reduced phosphorylation of AKT and p38, whereas cells treated with SN-38 were no longer responsive and thus considered resistant to SN-38. These results provide support for the design expectation that **K1** would produce an anti-cancer therapeutic response under conditions of both oxidative and reductive stress, with simultaneous reduction of intracellular oxidants/antioxidant levels as outlined in Figures 1A and 3E. We also compared the cytotoxicity of **K1** with other controls (DMSO, SN-38 only, indomethacin only, SN-38 + indomethacin) in SW620 cancer cells (Figure S12). It was found that **K1** exhibited improved toxicity relative other tested controls. Specifically, it proved 5-fold more potent than SN-38 alone and 3-fold more active than the combination of SN-38 and indomethacin (Table S1).

To determine whether the anti-inflammatory effect from the indomethacin moiety in **K1** was mediated by COX-2 inhibition, we evaluated the change in COX-2 activity by detecting PGE<sub>2</sub> levels in **K1**-treated cancer cells having variable COX-2 expression by means of an ELISA assay.<sup>40</sup> As shown in Figure 4A, **K1** effects strong attenuation of PGE<sub>2</sub> expression only in cancer cells having high COX-2 expression levels (LoVo and SW620 cells) but not in cells characterized by low COX-2 expression levels (Caco-2 and DLD1 Cells). We further observed that treatment with **K1**, but not SN-38, effectively decreased the PGE<sub>2</sub> level in SW620 cells in response to external lipopolysaccharide (LPS) mediated stimulation (Figure 4B).

To escape from immune surveillance, cancer cells often coalesce with cancer-associated immune cells and pro-inflammatory cytokines, such as interleukin-6 (IL-6) and tumor necrosis factor- $\alpha$  (TNF- $\alpha$ ), which are induced by tumor-associated macrophages.<sup>41</sup> This inflammatory microenvironment provides growth and survival advantages for cancer cells and enhances tumor cell resistance towards chemotherapies through activation of the NF- $\kappa$ B signaling pathway.<sup>42</sup> We thus sought to determine whether **K1** inhibited NF- $\kappa$ B activation and its target gene expression in SW620 cancer cells and RAW264.7 macrophages. Semi-quantitative RT-PCR analyses revealed that **K1** treatment suppressed the expression of NF- $\kappa$ B target genes, such as IL-6, TNF- $\alpha$ , and vascular endothelial growth factor (VEGF) in both a time- and dose-dependent manner (Figure 4C). In particular, **K1** exerted a strong inhibitory effect on LPS activation of these NF- $\kappa$ B target genes in both cancer cells and macrophages (Figure 4D). Moreover, immunoblot analysis of a major NF- $\kappa$ B component p65 and its regulator I $\kappa$ B $\alpha$  revealed that **K1** treatment inhibited the phosphorylation of both p65 and I $\kappa$ B $\alpha$ , again in a time- and dose-associated manner (Figure 4E). We also examined the effect of **K1** on inflammatory cytokine production using the enzyme-linked immunosorbent assay (ELISA) in RAW264.7 macrophages. As shown in Figure 4F, **K1**, but not SN-38, decreased in a statistically significant manner the production of the pro-inflammatory cytokines IL-6 and TNF- $\alpha$  while increasing production of the anti-inflammatory cytokine, IL-10.

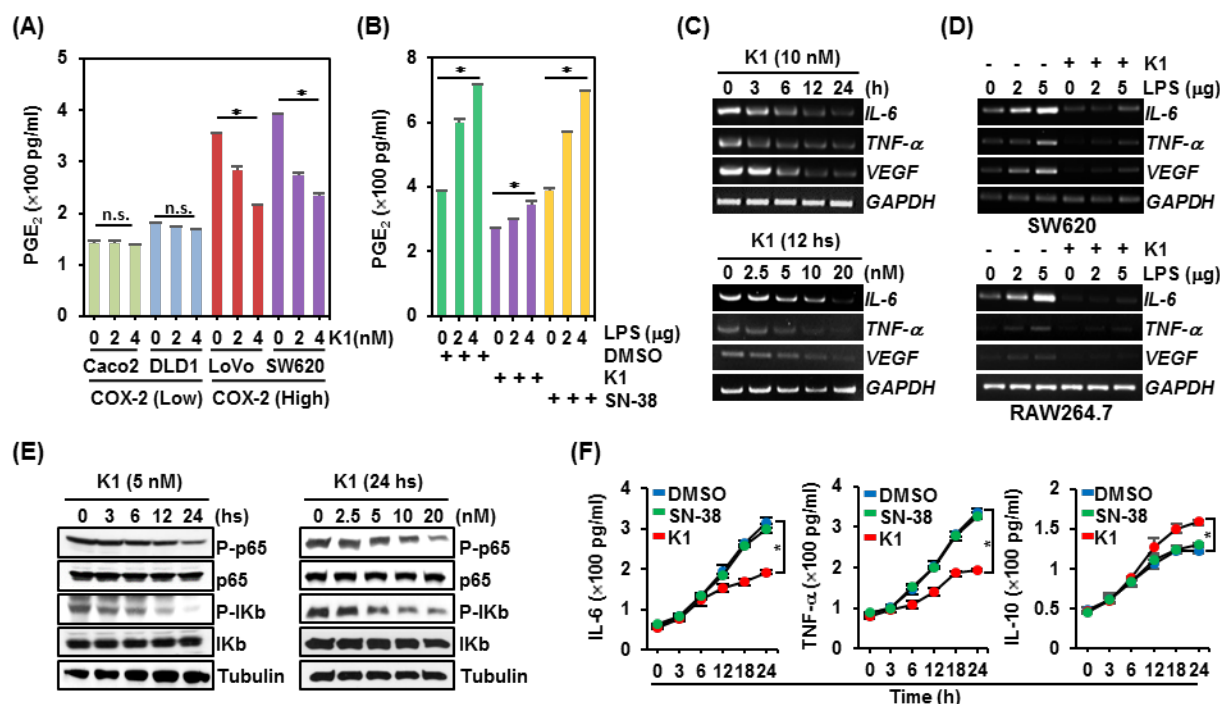


**Figure 4.** Anti-inflammatory effects of **K1**. (A) Comparison of PGE<sub>2</sub> levels in COX-2 low- or high-expressing cancer cells upon **K1** treatment. The levels of secreted PGE<sub>2</sub> were determined using an ELISA assay (mean ± SD, n = 3, \* p < 0.01, n.s., not significant). (B) Effect of **K1** on LPS-induced PGE<sub>2</sub> secretion in SW620 colon cancer cells. (C) Dose and time-associated effects of **K1** on IL-6, TNF-α, and VEGF mRNA expression levels in SW620 cells. (D) Effect of **K1** on LPS-induced IL-6, TNF-α, and VEGF mRNA expression levels in SW620 cancer cells and RAW264.7 mouse macrophage cells. (E) Time and dose-dependent effects of **K1** on the NF-κB signaling pathway. (F) ELISA detection of IL-6, TNF-α, and IL-10 in RAW264.7 cells in response to SN-38, **K1** or DMSO as vehicle control (mean ± SD of triplicate assays). \*p < 0.01 (Student's t-test).

In order to evaluate the tumor target specificity of the drug released from **K1** *in vivo*, nude mice bearing SW620 colon cancer subcutaneous xenografts were subjected to *in vivo* fluorescence image analysis 3 hours after administration of the agent. As shown in Figure 5A, the fluorescence signal of drug released from **K1** was observed in the xenograft tumor of **K1**-treated mice, while the fluorescence images of the excised organs displayed no such fluorescence signal (Figure 5A). To correlate the biological therapeutic effect with that of the *in vitro* cancer cell-based studies discussed above, we further assessed the efficacy of **K1** and SN-38 in nude mice bearing SW620 xenografts. Compared with DMSO, a mild response to SN-38 treatment was seen (20% tumor reduction), while **K1**-treated tumors displayed improved suppression of tumor growth (41% reduction) (Figure 5B-D, Figure S13). No significant weight loss was observed during any course of treatment (Figure S14). Also, aspartate transaminase (AST), alanine transaminase (ALT) and serum creatine levels in the blood serum of mice treated with **K1** remained in the normal range over the course of treatment (Figures S15 and S16). In contrast, test groups treated with SN-38 showed higher serum levels of AST and ALT. Additionally, we examined the effects of **K1** on tumor survival cytokine gene expression using xenograft tumor tissues. **K1** induced a significant reduction in the TNF-α, IL-6, and VEGF gene expression levels as compared to DMSO or SN-38 (Figure 5E). Taken in concert, these findings provide support for the conclusion that treatment with **K1** provides for improved antitumor efficacy relative to controls, as evidenced by both tumor regrowth analyses and the observed selective suppression of cancer survival cytokine expression.

## CONCLUSIONS

In summary, we have developed **K1**, a molecular-based system that targets cancers with COX-2 overexpression and which is activated intracellularly by reductive and oxidative stress expected to exist in various cancerous microenvironment. This activation serves to release the active drug SN-38. Redox mediated activation of the prodrug not only allows for release of the active drug SN-38, it also scavenges the corresponding biomolecules (GSH, H<sub>2</sub>O<sub>2</sub>) so as to downregulate alternative cell survival signaling pathways. The indomethacin moiety incorporated into **K1** serves to knockdown inflammatory responses mediated by COX-2 and is thought to contribute to the improved efficacy seen for this agent relative to controls. Operationally, **K1** proved capable of inhibiting tumor growth to greater extent than the FDA approved drug SN-38, with no significant side effects as inferred from liver function assays, analyses of blood markers, and body weight measurements. Detailed toxicological analyses of **K1** are ongoing and will be reported in due course.

The current investigation provides support for the notion that small, molecular-based drug delivery systems that have the potential to release an active drug form under conditions of both oxidative and reductive stress may lead to improvements in efficacy as determined from *in vitro* analyses and mouse model studies. It thus sets the stage for the further development of targeted therapies for use in addressing the heterogeneous tumor microenvironments that make the development of improved cancer therapeutics challenging.

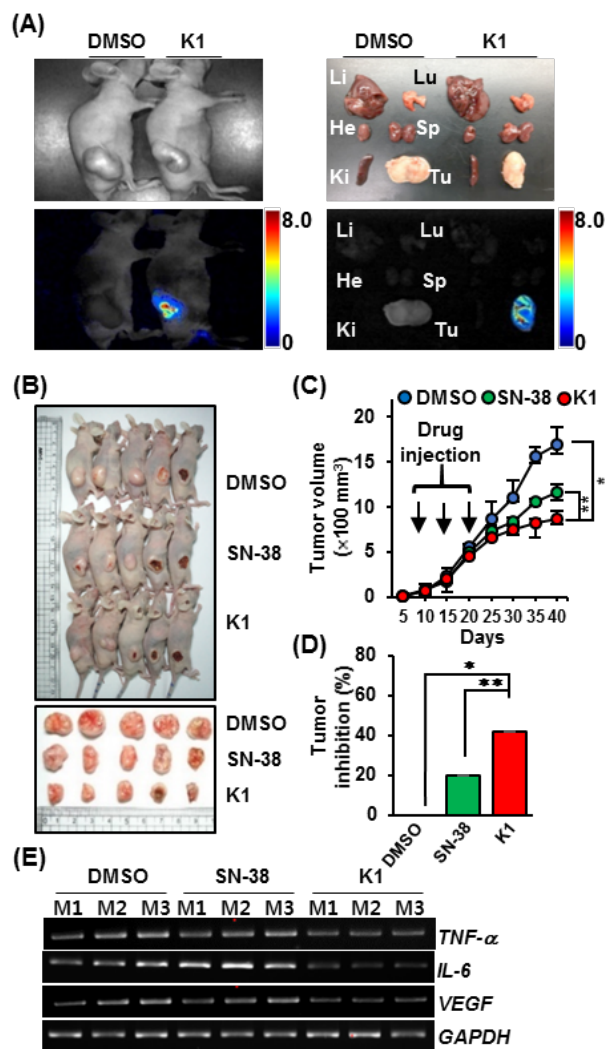


**Figure 5.** *In vivo* therapeutic efficacy of **K1** in tumor xenografts. (A) Representative fluorescence images of mice bearing SW620 tumors and *ex vivo* images of dissected organs. Li = liver, Lu = lung, He = heart, Sp = spleen, Ki = kidney, Tu = tumor. (B) Representative images of SW620 xenograft tumors treated with control (DMSO), SN-38, and **K1**. (C) **K1**-induced regression of tumors ( $n = 5$  per group, mean  $\pm$  SD, \*  $p < 0.01$ , \*\*  $p < 0.05$ ). (D) Tumor inhibition levels determined from sacrificed mice following treatment with DMSO, SN-38, or **K1**, \*  $p < 0.05$  and \*\*  $p < 0.01$ ,  $n = 5$ /group. Tumor inhibition rate (%) =  $100 - (\text{tumor weight of treatment} / \text{tumor weight of DMSO}) \times 100$  (E) Anti-inflammatory cytokine mRNA levels of the mice in the DMSO control, SN-38, and **K1** treated tissue (mean  $\pm$  SD), \*  $p < 0.05$ , \*\*  $p < 0.01$ ).

## ■ ASSOCIATED CONTENT

### Supporting Information

The Supporting Information is available free of charge on the ACS Publications website. Detailed experiment procedures and supporting figures (PDF). This material is available free of charge via the Internet at <http://pubs.acs.org>.

## ■ AUTHOR INFORMATION

### Corresponding Author

\*chi6302@korea.ac.kr (S.-G.C.)

\*sessler@utexas.edu (J.L.S.)

\*jongskim@korea.ac.kr (J.S.K.)

### Author Contributions

† These authors contributed equally.

### Notes

The authors declare no competing financial interest.

## ■ ACKNOWLEDGMENTS

This work was supported in part by a Creative Research Initiatives project (grant no. 2018R1A3B1052702, J.S.K.) and a grant from the National Research Foundation of Korea (NRF-2018R1A2A1A05020236, S.-G.C.) and 2017R1D1A1B03030062, M.W.). Funding from the National Cancer Institute (RO1 CA68682, J.L.S. and R15 CA232765, J.F.A.) and the Robert A. Welch Foundation (F-0018, J.L.S.) is also acknowledged.

## ■ REFERENCES

- (1) Hay, M.; Thomas, D. W.; Craighead, J. L.; Economides, C.; Rosenthal, J. Clinical development success rates for investigational drugs. *Nat. Biotechnol.* **2014**, *32*, 40-51.
- (2) Hanahan, D.; Weinberg, R. A. Hallmarks of cancer: the next generation. *Cell* **2011**, *144*, 646-674.
- (3) Allen, T. M., Ligand-targeted therapeutics in anticancer therapy. *Nat. Rev. Cancer* **2002**, *2*, 750-63.
- (4) Sharma, A.; Arambula, J. F.; Koo, S.; Kumar, R.; Singh, H.; Sessler, J. L.; Kim, J. S. Hypoxia-targeted drug delivery. *Chem. Soc. Rev.* **2019**, *48*, 771-813.
- (5) Merkel, T. J.; DeSimone, J. M., Dodging drug-resistant cancer with diamonds. *Sci. Transl. Med.* **2011**, *3*, 73ps8.
- (6) Sharma, A.; Lee, M. G.; Shi, H.; Won, M.; Arambula, J. F.; Sessler, J. L.; Lee, J. Y.; Chi, S. G.; Kim, J. S. Overcoming Drug Resistance by Targeting Cancer Bioenergetics with an Activatable Prodrug. *Chem-U.S.* **2018**, *4*, 2370-2383.
- (7) Lee, M. H.; Sharma, A.; Chang, M. J.; Lee, J.; Son, S.; Sessler, J. L.; Kang, C.; Kim, J. S. Fluorogenic reaction-based prodrug conjugates as targeted cancer theranostics. *Chem. Soc. Rev.* **2018**, *47*, 28-52.
- (8) Gnaim, S.; Scamparin, A.; Das, S.; Blau, R.; Satchi-Fainaro, R.; Shabat, D. Direct real-time monitoring of prodrug activation by chemiluminescence. *Angew. Chem. Int. Ed.* **2018**, *57*, 9033-9037.
- (9) McCawley, L. J.; Matrisian, L. M. Matrix metalloproteinases: multifunctional contributors to tumor progression. *Mol. Med. Today* **2000**, *6*, 149-156.
- (10) Dong, Z.; Feng, L.; Chao, Y.; Hao, Y.; Chen, M.; Gong, F.; Han, X.; Zhang, R.; Cheng, L.; Liu, Z. Amplification of Tumor Oxidative Stresses with Liposomal Fenton Catalyst and Glutathione Inhibitor for Enhanced Cancer Chemotherapy and Radiotherapy. *Nano Lett.* **2019**, *19*, 805-815.
- (11) Hamburg, M. A. Science and regulation. FDA's approach to regulation of products of nanotechnology. *Science* **2012**, *336*, 299-300.
- (12) Zhang, Y.; Chan, H. F.; Leong, K. W. Advanced materials and processing for drug delivery: the past and the future. *Adv. Drug Deliv. Rev.* **2013**, *65*, 104-120.
- (13) Siegel, R. L.; Miller, K. D.; Fedewa, S. A.; Ahnen, D. J.; Meester, R. G. S.; Barzi, A.; Jemal, A. Colorectal cancer statistics, 2017. *CA: Cancer J. Clin.* **2017**, *67*, 177-193.
- (14) van der Geest, L. G.; Lam-Boer, J.; Koopman, M.; Verhoef, C.; Elferink, M. A.; de Wilt, J. H. Nationwide trends in incidence, treatment and survival of colorectal cancer patients with synchronous metastases. *Clin. Exp. Metastasis* **2015**, *32*, 457-465.
- (15) Markman, J. L.; Shiao, S. L. Impact of the immune system and immunotherapy in colorectal cancer. *J. Gastrointest. Oncol.* **2015**, *6*, 208-223.
- (16) Slatter, J. G.; Schaaf, L. J.; Sams, J. P.; Feenstra, K. L.; Johnson, M. G.; Bombardt, P. A.; Cathcart, K. S.; Verburg, M. T.; Pearson, L. K.; Compton, L. D.; Miller, L. L.; Baker, D. S.; Pesheck, C. V.; Lord, R. S. 3rd, Pharmacokinetics, metabolism, and excretion of irinotecan

(CPT-11) following I.V. infusion of [(14)C]CPT-11 in cancer patients. *Drug Metab. Dispos.* **2000**, *28*, 423-433.

(17) de Man, F. M.; Goey, A. K. L.; van Schaik, R. H. N.; Mathijssen, R. H. J.; Bins, S. Individualization of Irinotecan Treatment: A Review of Pharmacokinetics, Pharmacodynamics, and Pharmacogenetics. *Clin. Pharmacokinet.* **2018**, *57*, 1229-1254.

(18) Nakanishi, M.; Rosenberg, D. W. Multifaceted roles of PGE2 in inflammation and cancer. *Semin. Immunopathol.* **2013**, *35*, 123-137.

(19) Zelenay, S.; van der Veen, A. G.; Bottcher, J. P.; Snelgrove, K. J.; Rogers, N.; Acton, S. E.; Chakravarty, P.; Girotti, M. R.; Marais, R.; Quezada, S. A.; Sahai, E.; Sousa, C. R. E. Cyclooxygenase-Dependent Tumor Growth through Evasion of Immunity. *Cell* **2015**, *162*, 1257-1270.

(20) Ogino, S.; Kirkner, G. J.; Nosho, K.; Irahara, N.; Kure, S.; Shima, K.; Hazra, A.; Chan, A. T.; Dehari, R.; Giovannucci, E. L.; Fuchs, C. S. Cyclooxygenase-2 Expression Is an Independent Predictor of Poor Prognosis in Colon Cancer. *Clin. Cancer Res.* **2008**, *14*, 8221-8227.

(21) Xu, L.; Stevens, J.; Hilton, M. B.; Seaman, S.; Conrads, T. P.; Veenstra, T. D.; Logsdon, D.; Morris, H.; Swing, D. A.; Patel, N. L.; Kalen, J.; Haines, D. C.; Zudaire, E.; St Croix, B. COX-2 inhibition potentiates antiangiogenic cancer therapy and prevents metastasis in preclinical models. *Sci. Transl. Med.* **2014**, *6*, 242ra84.

(22) Kim, H. S.; Sharma, A.; Ren, W. X.; Han, J.; Kim, J. S. COX-2 Inhibition mediated anti-angiogenic activatable prodrug potentiates cancer therapy in preclinical models. *Biomaterials* **2018**, *185*, 63-72.

(23) Zhang, H.; Fan, J. L.; Wang, J. Y.; Zhang, S. Z.; Dou, B. R.; Peng, X. J., An Off-On COX-2-Specific Fluorescent Probe: Targeting the Golgi Apparatus of Cancer Cells. *J. Am. Chem. Soc.* **2013**, *135*, 11663-11669.

(24) Zhang, H.; Fan, J.; Wang, J.; Dou, B.; Zhou, F.; Cao, J.; Qu, J.; Cao, Z.; Zhao, W.; Peng, X., Fluorescence discrimination of cancer from inflammation by molecular response to COX-2 enzymes. *J. Am. Chem. Soc.* **2013**, *135*, 17469-17475.

(25) Uddin, M. J.; Crews, B. C.; Ghebreselasie, K.; Marnett, L. J., Design, synthesis, and structure-activity relationship studies of fluorescent inhibitors of cyclooxygenase-2 as targeted optical imaging agents. *Bioconjug. Chem.* **2013**, *24*, 712-723.

(26) Uddin, M. J.; Crews, B. C.; Ghebreselasie, K.; Daniel, C. K.; Kingsley, P. J.; Xu, S.; Marnett, L. J., Targeted imaging of cancer by fluorocoxib C, a near-infrared cyclooxygenase-2 probe. *J. Biomed. Opt.* **2015**, *20*, 50502.

(27) Visvader, J. E. Cells of origin in cancer. *Nature* **2011**, *469*, 314-322.

(28) Marusyk, A.; Polyak, K. Tumor heterogeneity: causes and consequences. *Biochim. Biophys. Acta* **2010**, *1805*, 105-117.

(29) Traverso, N.; Ricciarelli, R.; Nitti, M.; Marengo, B.; Furfaro, A. L.; Pronzato, M. A.; Marinari, U. M.; Domenicotti, C. Role of glutathione in cancer progression and chemoresistance. *Oxid. Med. Cell Longev.* **2013**, *2013*, 972913.

(30) Szatrowski, T. P.; Nathan, C. F., Production of large amounts of hydrogen peroxide by human tumor cells. *Cancer Res.* **1991**, *51*, 794-798.

(31) Reuter, S.; Gupta, S. C.; Chaturvedi, M. M.; Aggarwal, B. B. Oxidative stress, inflammation, and cancer: how are they linked? *Free Radic. Biol. Med.* **2010**, *49*, 1603-1616.

(32) Huo, M.; Yuan, J.; Tao, L.; Wei, Y. Redox-responsive polymers for drug delivery: from molecular design to applications. *Polym. Chem.-Uk* **2014**, *5*, 1519-1528.

(33) Lyu, Y.; Tian, J.; Li, J.; Chen, P.; Pu, K. Semiconducting polymer nanobiocatalysts for photoactivation of intracellular redox reactions. *Angew. Chem. Int. Ed.* **2018**, *57*, 13484-13488.

(34) Napoli, A.; Valentini, M.; Tirelli, N.; Muller, M.; Hubbell, J. A. Oxidation-responsive polymeric vesicles. *Nat. Mater.* **2004**, *3*, 183-189.

(35) Yang, W.; Gao, X.; Wang, B. Boronic Acids: Biological and Medical Applications of Boronic Acids; Hall, D. G., Ed.; Wiley-VCH Verlag GmbH & Co. KGaA: Weinheim, **2005**, p 481-512.

(36) Austin, C. D.; Wen, X.; Gazzard, L.; Nelson, C.; Scheller, R. H.; Scales, S. J. Oxidizing potential of endosomes and lysosomes limits intracellular cleavage of disulfide-based antibody-drug conjugates. *Proc. Natl. Acad. Sci. U S A* **2005**, *102*, 17987-17992.

(37) Che, X. H.; Chen, C. L.; Ye, X. L.; Weng, G. B.; Guo, X. Z.; Yu, W. Y.; Tao, J.; Chen, Y. C.; Chen, X., Dual inhibition of COX-2/5-LOX blocks colon cancer proliferation, migration and invasion in vitro. *Oncol. Rep.* **2016**, *35*, 1680-1688.

(38) Liu, Y.; Li, Q.; Zhou, L.; Xie, N.; Nice, E. C.; Zhang, H.; Huang, C.; Lei, Y., Cancer drug resistance: redox resetting renders a way. *Oncotarget* **2016**, *7*, 42740-42761.

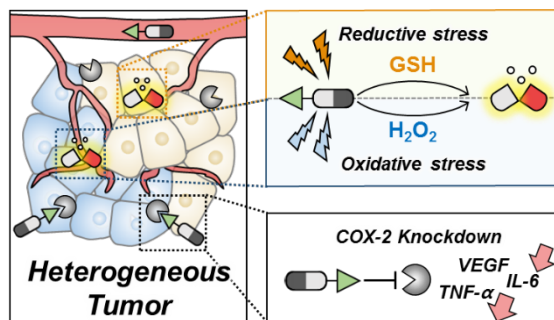
(39) Moldogazieva, N. T.; Lutsenko, S. V.; Terentiev, A. A. Reactive Oxygen and Nitrogen Species-Induced Protein Modifications: Implication in Carcinogenesis and Anticancer Therapy. *Cancer Res.* **2018**, *78*, 6040-6047.

(40) Cuendet, M.; Mesecar, A. D.; DeWitt, D. L.; Pezzuto, J. M., An ELISA method to measure inhibition of the COX enzymes. *Nat. Protoc.* **2006**, *1*, 1915-1921.

(41) Gonzalez, H.; Hagerling, C.; Werb, Z. Roles of the immune system in cancer: from tumor initiation to metastatic progression. *Genes Dev.* **2018**, *32*, 1267-1284.

(42) Ratnam, N. M.; Peterson, J. M.; Talbert, E. E.; Ladner, K. J.; Rajasekera, P. V.; Schmidt, C. R.; Dillhoff, M. E.; Swanson, B. J.; Haverick, E.; Kladney, R. D.; Williams, T. M.; Leone, G. W.; Wang, D. J.; Guttridge, D. C. NF- $\kappa$ B regulates GDF-15 to suppress macrophage surveillance during early tumor development. *J. Clin. Invest.* **2017**, *127*, 3796-3809.

### Table of Contents



1  
2  
3  
4  
5  
6  
7  
8  
9  
10  
11  
12  
13  
14  
15  
16  
17  
18  
19  
20  
21  
22  
23  
24  
25  
26  
27  
28  
29  
30  
31  
32  
33  
34  
35  
36  
37  
38  
39  
40  
41  
42  
43  
44  
45  
46  
47  
48  
49  
50  
51  
52  
53  
54  
55  
56  
57  
58  
59  
60